

A Vibration Mission Synthesis Algorithm for Mildly Nonstationary Road Data

J. Giacomini, A. Steinwolf, W. J. Staszewski

Department of Mechanical Engineering, The University of Sheffield
Mappin Street, Sheffield S1 3JD, UK

Abstract

This paper describes a mission synthesis algorithm developed for producing short test signal sequences which are representative of road data records. The algorithm is based on the use of Fourier analysis, orthogonal Daubechies 12 wavelets, and peak correction procedures. Crest factor control with consideration of kurtosis value of the signal provides realistic signal sequences for comfort testing due to the close correspondence between these statistics and the metrics used for evaluation of human comfort such as the vibration dose value (VDV). Signal compression ratios of up to 8 have been achieved.

1. Introduction

An important technical problem associated with the design, development and testing of vehicle subsystems is the definition of the operating conditions which the system will face when in use. The situation is critical in the field of automotive NVH, where numerous components and subsystems are nonlinear, providing significantly different vibratory behaviour depending on the nature of the input excitation provided to the system. An example of a typical nonlinear vehicle component is the person/seat system. Seat transmissibility measurements show a softening system behaviour, with the principal resonance shifting to lower frequencies as the excitation amplitude at the base of the seat rises [3]. Industrial testing methods such as those applied to seats normally work around the problem of nonlinearity by using several test signals [2]. These mission signals either correspond directly to measured operating conditions, or they are formed from selected portions of the road inputs which are considered critical to successful vehicle performance based on the previous experiences of the test engineers involved. Mission signal definition constitutes a technical challenge, and an important step in the design and development process.

In the durability area, several algorithms are available to analyse road data for the purpose of synthesising excitation signals for fatigue testing. Concepts such as rainflow counting, or techniques based on the Weibull distribution have been successfully applied. No such algorithms have been developed for the purpose of NVH testing, or more specifically, human comfort testing such as in the case of seats. This paper presents an algorithm developed at the University of Sheffield for performing vibration mission synthesis of mildly nonstationary vibration signals. The algorithm is based on the use of the Fourier Transform, the Orthogonal Wavelet Transform [1,4,5] and simple peak correcting techniques. The software provides short data segments, or mission signals, which are representative of the original long road data record in several statistical metrics including: power spectral density, probability density function, crest factor and kurtosis. Crest factor control with consideration of kurtosis value provides realistic signal sequences for comfort testing due to the close correspondence between these statistics and the metrics used for evaluating human comfort such as the vibration dose value (VDV). This research was carried out as part of European Union Project BE-97-4186 SCOOP which is developing an experimental seat comfort testing procedure. Within the project, the algorithm provides the means for defining the short test signals starting from large quantities of measured road data.

2. Classification of road data

The experimental road data used during this study consisted of vertical acceleration records measured at the rear mounting bolt of the left guide of the driver's seat of a Renault automobile. There were 11 different road tracks of four types: speed circuit, highway, good road, country road and pave road. Each of the records represented steady-state vehicle motion of more than a minute time length when a driver was trying to keep vehicle speed and all other controls constant. It is a common assumption that vehicle vibration signals measured under such conditions can be considered as stationary Gaussian random process and, therefore, completely described by power spectral density (PSD) which characterises distribution of vibration energy in the frequency domain.

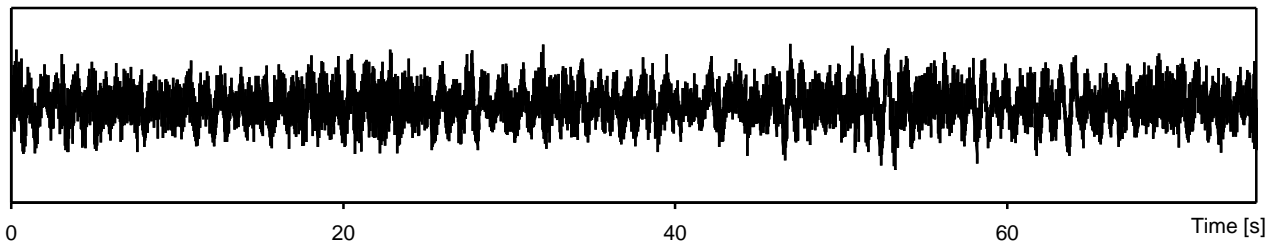
However, even preliminary analysis of the available data transferred to digital form with a sampling rate of 409.6 Hz has shown that only 2 of all 11 records followed the above assumption. An example of such kind is the highway vibration presented in Fig. 1,a. There are three parameters describing deviations from the Gaussian stationary model: skewness that is an average of vibration instantaneous values $x(j\Delta t)$ cubed

$$\lambda = L^{-1} \sigma^{-3/2} \sum_{j=1}^L x^3(j\Delta t) \quad (1)$$

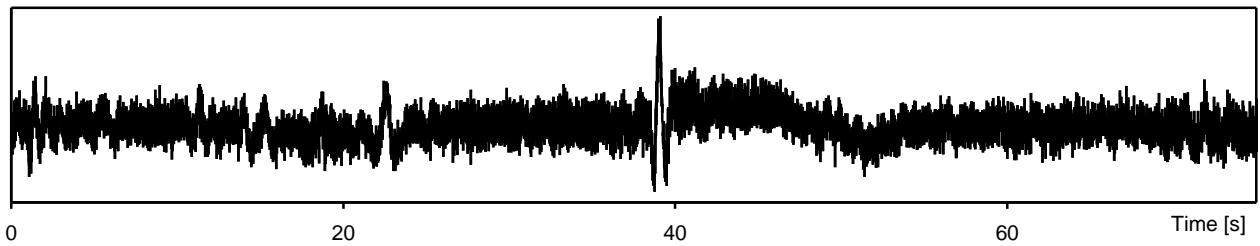
kurtosis that is a similar character involving the fourth power and, consequently, sensitive to outlying points among instantaneous values

$$\gamma = L^{-1} \sigma^{-2} \sum_{j=1}^L x^4(j\Delta t) \quad (2)$$

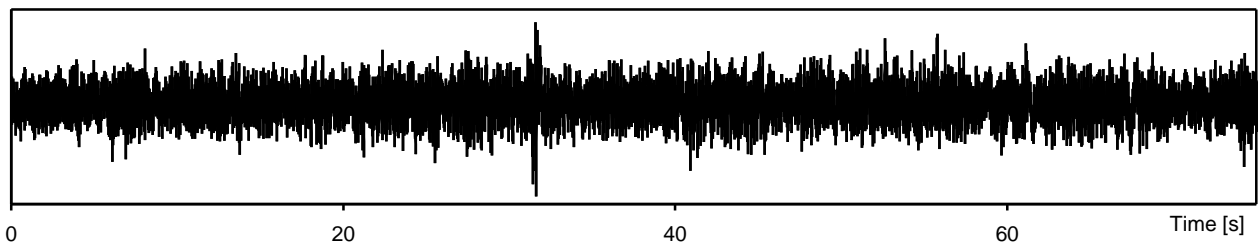
and crest factor c that is a ratio between time history maximum and root-mean-square (RMS) value of the signal $\sigma = \left\{ L^{-1} \sum_{j=1}^L x^2(j\Delta t) \right\}^{-1/2}$. For the highway vibration and one other similar record, the skewness, kurtosis and crest factor have acquired values (see caption to Fig. 1,a) close to those $\lambda = 0$, $\gamma = 3.0$, $3.5 < c < 4.0$ inherent of Gaussian stationary processes.



a) Stationary Gaussian random signal with $\lambda = 0.04$, $\gamma = 3.04$, $c = 3.9$ (highway road)



b) Heavy nonstationary signal (good road with a climb)



c) Mildly nonstationary signal with $\lambda = 0.01$, $\gamma = 3.23$, $c = 5.9$ (speed circuit road)

Fig. 1 Time histories of vertical acceleration measured in the Renault automobile

Among the remaining 9 records which failed to match Gaussian model there were 2 records with obvious nonstationary behaviour like that in Fig. 1,b having variable frequency content, RMS and mean value. Except these heavy nonstationary signals all other data can be classified as mildly nonstationary vibration. *This definition means a random vibration process with stable mean and RMS values most of the record but containing a few high peaks due to transients and shocks.* The high peaks correspond to bump events when a vehicle moves over considerable separate irregularity such as a pot-hole. An example of mildly nonstationary vibration is presented in Fig. 1,c and high time history peaks like that visible on the plot are reflected in increase of kurtosis and crest factor up to $\gamma = 3.23$ and $c = 5.9$ values correspondingly.

3. Vibration mission synthesis procedure

Since vibration of mildly nonstationary type prevailed in the road nonstationary data analysed (approximately 65 % of the recorded data), effort has been invested towards establishing a procedure for vibration mission synthesis appropriate for this type of road data. The approach was to establish a numerical simulation algorithm in three stages. First, the background vibration was generated in the form of Fourier expansion with a large number N of harmonics

$$y(t) = \sum_{k=1}^N A_k \cos(2\pi k \Delta f t + \varphi_k). \quad (3)$$

This is a basic procedure [8,9] used in digital random controllers for shakers and similar test benches. In so doing one can reproduce stationary Gaussian random excitations in frequency domain matching precisely the PSD of road data prescribed. The latter is attained when amplitudes are determined

$$A_k = \sqrt{2\Delta f S(k\Delta f)} \quad (4)$$

by the PSD values $S(f)$ corresponding to frequencies $k\Delta f$ of harmonic components in formula (3). The phase angles φ_k are chosen in a random manner making the background time history (3) of the vibration mission to be also of random nature. Thus, at the end of the first stage one has a stationary Gaussian vibration mission with a power spectrum of the mildly nonstationary road data prescribed.

Of course, at that point, bump events occurring in the road data are not present in the vibration mission. The second stage of the algorithm is to identify those moments in the road time history when it behaves differently from a Gaussian random process producing high peaks like that shown in Fig. 1,c. If all such bump events are collected and, then on the third stage, introduced in some way to the mission background vibration obtained on the above first stage, the upgraded mission signal becomes mildly nonstationary in nature. A flow-chart of the whole procedure of vibration mission synthesis is presented in Fig. 2 and 3.

The main difficulty on the second stage of extracting bump events lies in the fact that most bumps are not so obvious in the road time history as one shown in Fig. 1,c. It is therefore helpful to separate the recorded road vibration into a number of components each of which is related to certain physical phenomenon happening during vehicle motion, e.g. resonance of the vehicle body as entire mass, torsion and bending of the frame in different directions, tire resonance, etc. If this is done and each of the component vibrations is considered separately, the bump events caused by one physical phenomenon will not be covered by background vibration related to another phenomenon.

Normally each physical phenomenon has its own frequency range and, therefore, can be distinguished by analyzing the power spectral density of road vibration. However, it is not so easy to actually separate one particular phenomenon and to obtain its own time history record. Separation is often performed by means of Butterworth or other band-pass digital filters, but since every point in the filtered output is affected by its neighbours, the filtering affects the time history by smoothing peaks. Moreover, if a number of band-pass outputs from the same input process are summarized back, the result will not be exactly the same time history which was subjected to filtering. This contradicts with the paper objective to reconstruct a vibration mission after consideration of bumps in the component processes. That is why wavelet decomposition, being a procedure which can be precisely reverted, has been chosen as a tool for separation of road vibration time history into components of different physical nature to be analyzed in terms of bump behaviour. How it was done is explained in the next section for a typical example of the real road data chosen according to classification made in the previous section.

4. Wavelet decomposition and comparison of road data with synthetic Fourier signal

Previous research by the authors [6,7] has shown that signal analysis and synthesis is facilitated if the original vibration time history is first decomposed by means of the orthogonal wavelet transform [1,4,5]. Wavelets are mathematical functions $\psi(t)$ which are used to decompose a signal $x(t)$ into scaled wavelet co-efficients $W_\psi(a,b)$. The continuous wavelet transform is a time-scale method which can be expressed as

$$W_\psi(a,b) = \int_{-\infty}^{\infty} x(t) \frac{1}{\sqrt{a}} \psi^* \left(\frac{t-b}{a} \right) dt \quad (5)$$

where $\psi_{a,b}^*(t)$ are the scaled wavelets and ψ^* is the complex conjugate of ψ . The basis wavelet $\psi(t)$ can be any of a number of functions which satisfy admissibility conditions [5]. A natural extension of continuous analysis is a discretisation of time b and scale a according to $a = a_0^m$, $b = na_0^n b_0$ where m and n are

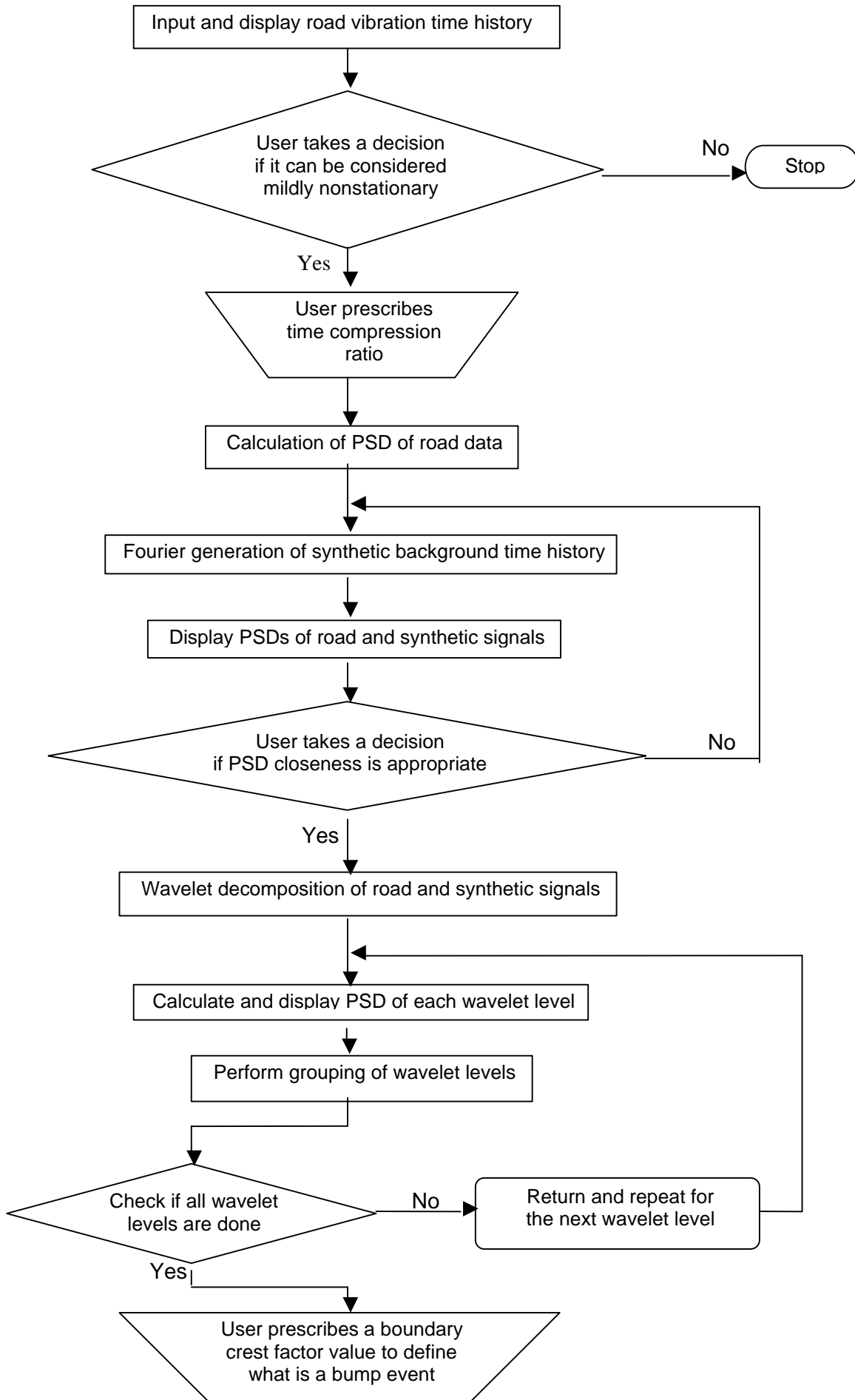


Fig. 2 Flow-chart of vibration mission synthesis algorithm (Fourier generation and wavelet grouping)

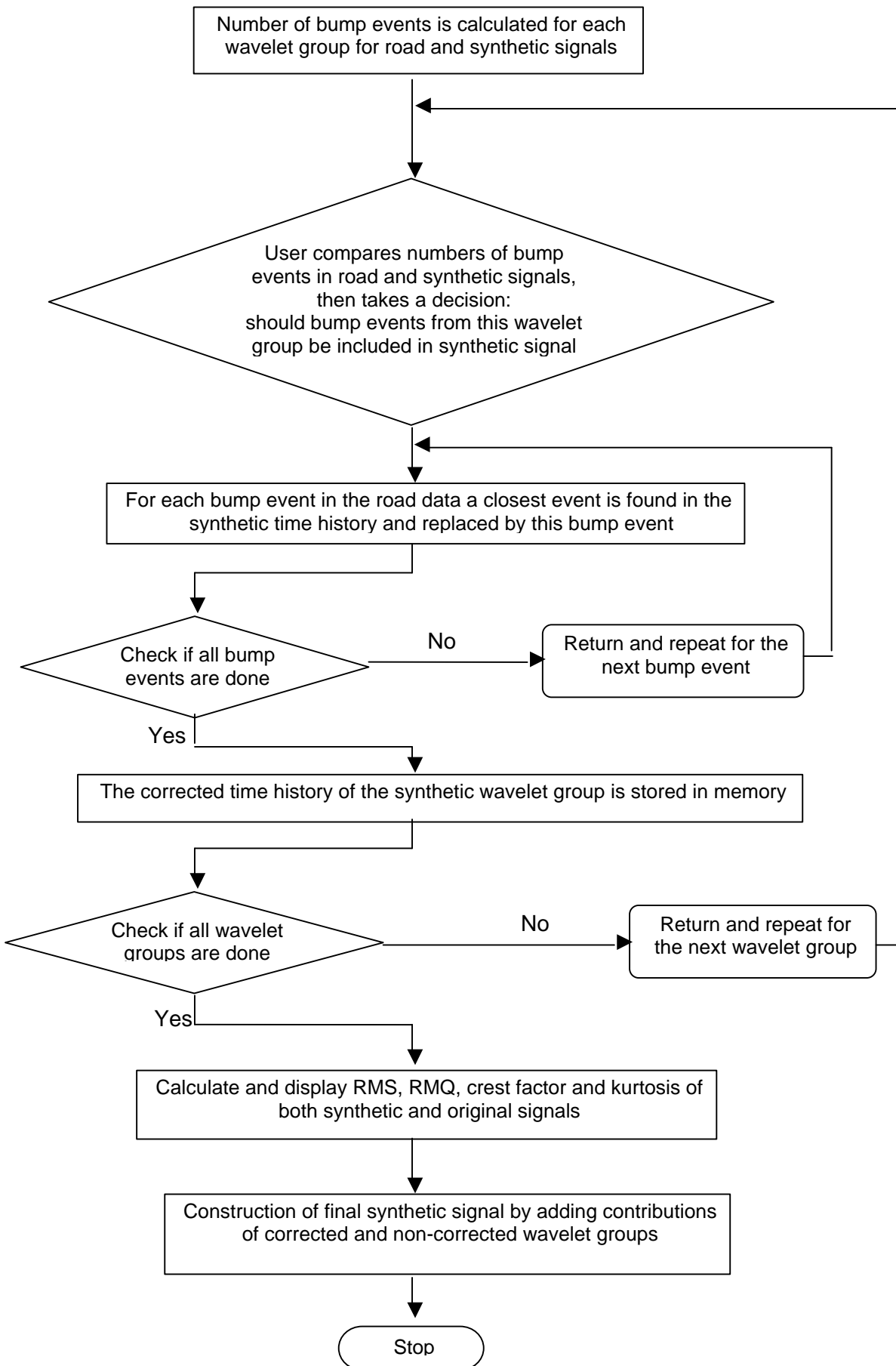


Fig. 3 Continuation of flow-chart of vibration mission synthesis algorithm (bump extraction, bump introduction, calculation of statistics and mission reconstruction)

integers, $b_0 \neq 0$ is the translation step. This implies a discretisation of the time-scale grid, and thus a discrete wavelet transform can be given by

$$W_\psi(m, n) = \int_{-\infty}^{\infty} x(t) a_0^{-m/2} \psi^*(a_0^{-m}, t - nb_0) dt$$

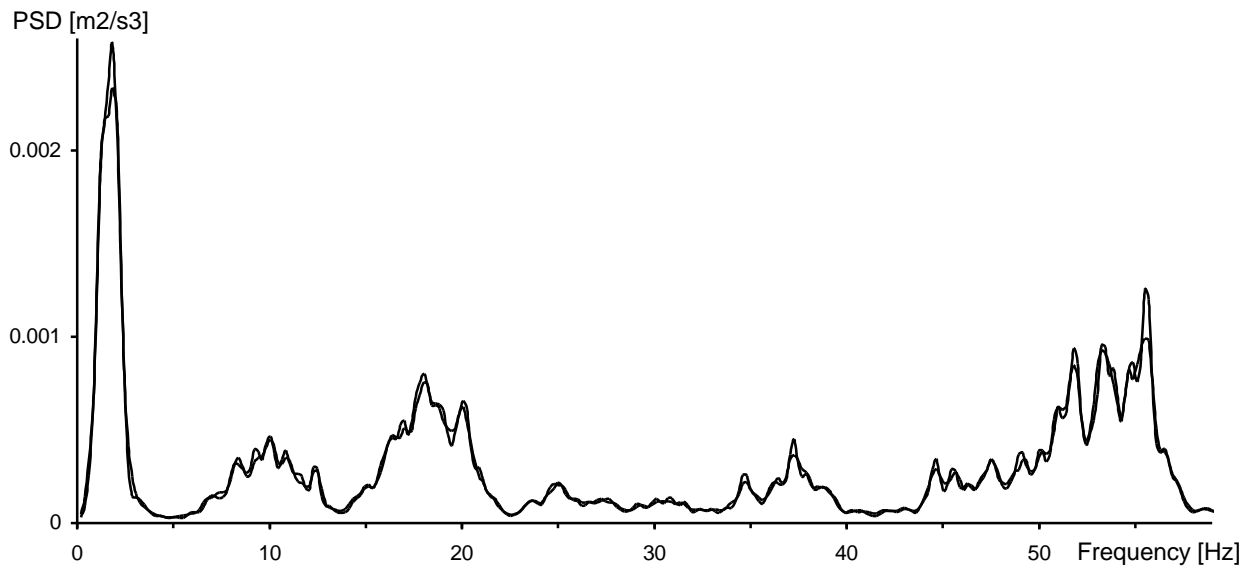
When the wavelets $\psi_{m,n}(t)$ form a set of orthonormal functions, there is no redundancy in the analysis. The discrete wavelet transform based on such wavelet functions is called the orthogonal wavelet transform. These transforms are particularly convenient in damage detection and other feature selection applications, and have thus been adopted as a basic component of the algorithm described in this paper. The algorithm makes use of wavelet levels which are reconstructed signals from the wavelet decomposition for a given value of scale a_0^{-m} . The 12th order of the Daubechies function was used in the analysis.

Power spectral density (Fig. 4,a) of one of the mildly nonstationary road data examples recorded in a Renault automobile on a country road included three distinguishable peaks at 1.8, 10 and 18 Hz with the rest of energy (more than 50%) spread at higher frequencies. The first peak with its slopes stretched in the region from 0.8 to 3.5 Hz can be associated with the rigid body motion of the car. The second peak covering from 5 to 14 Hz relates to suspension resonances and the rigid body motion of the engine/gearbox. The third peak distributed between 14 and 22 Hz reflects mainly the first flexible body resonance of the chassis and the fourth broadest region including frequencies from 23 to 58 Hz is defined by higher chassis resonances and tire resonances. Having in mind as an objective to separate these four physical phenomena and to obtain for each its own time history one should first calculate PSDs of all wavelet levels and present them on the same scale. Each of the levels corresponds to certain frequency range and retains all time domain features related to the bump events in the entire road data recorded. The wavelet levels should then be grouped in such a way that each group corresponds to one of the frequency-band sections of the whole PSD. Some groups will combine several wavelet levels while others will consist of only one wavelet level.

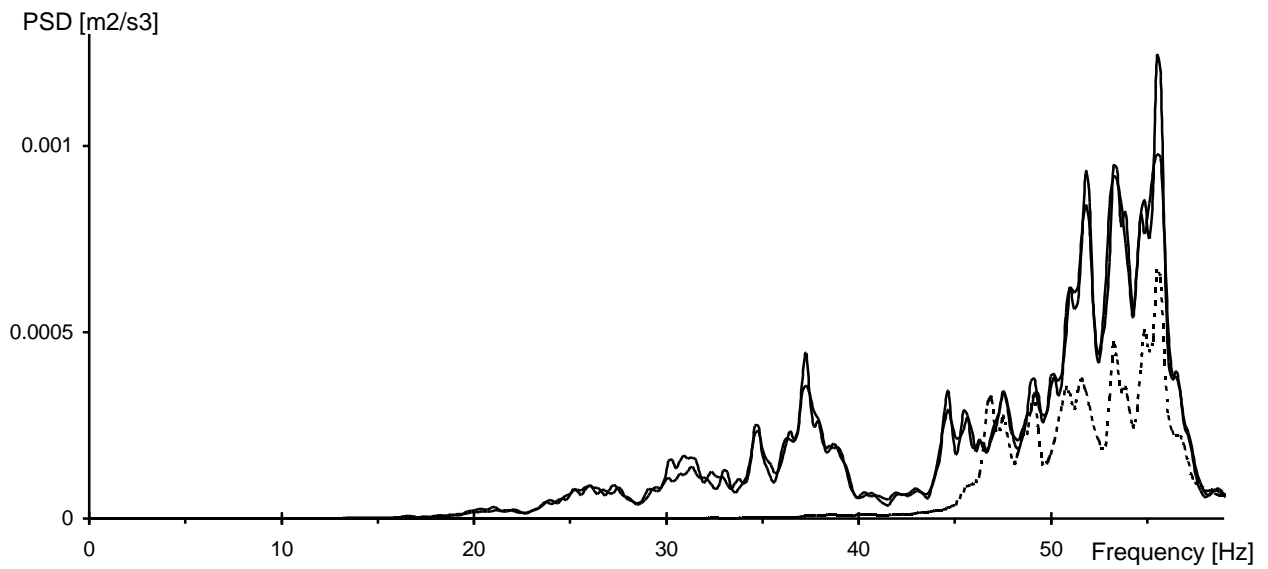
In the example under consideration the road data file included about 30000 points that means existence of 15 wavelet levels which are counted in the direction from high to low frequencies. The 1st level with highest frequencies fell to the right of the last fourth PSD section in Fig. 4,a and, therefore, has not been taken for further analysis. The 2nd and 3rd wavelet levels having PSDs presented in Fig. 4,b,c by dotted curves made up wavelet group No 1 whose PSD (solid curve in Fig. 4,c) fits fourth section from 23 to 58 Hz of the initial road data PSD. The 4th and 5th wavelet levels each separately matched third (from 14 to 22 Hz) and second (from 5 to 14 Hz) peak sections of the road data PSD. Thus, the 4-th level was designated as wavelet group No 2 and the 5th level – as wavelet group No 3. The 6th wavelet level, much smaller than preceding ones, has not been included in any of the groups because its frequency range appeared to be located between first (from 0.4 to 4 Hz) and second (from 5 to 14 Hz) sections of the road data PSD. The last wavelet group No 4 consisted of 7th and 8th levels. All further wavelet levels starting from 9th were omitted because their frequency regions are located lower than the lowest present frequency in the road data PSD.

The same wavelet grouping was performed for the synthetic data file generated according to (3). Power spectral density for wavelet group No 1 constructed for this synthetic signal as well as its entire PSD are also presented in Fig. 4,b,a for comparison with corresponding curves of road data. It is clear from this comparison and from similar results for other wavelet groups that the synthetic background signal has precisely acquired all frequency content features not only for PSD of the entire signal but also separately for each of four PSD of the wavelet groups obtained by wavelet decomposition of this entire signal.

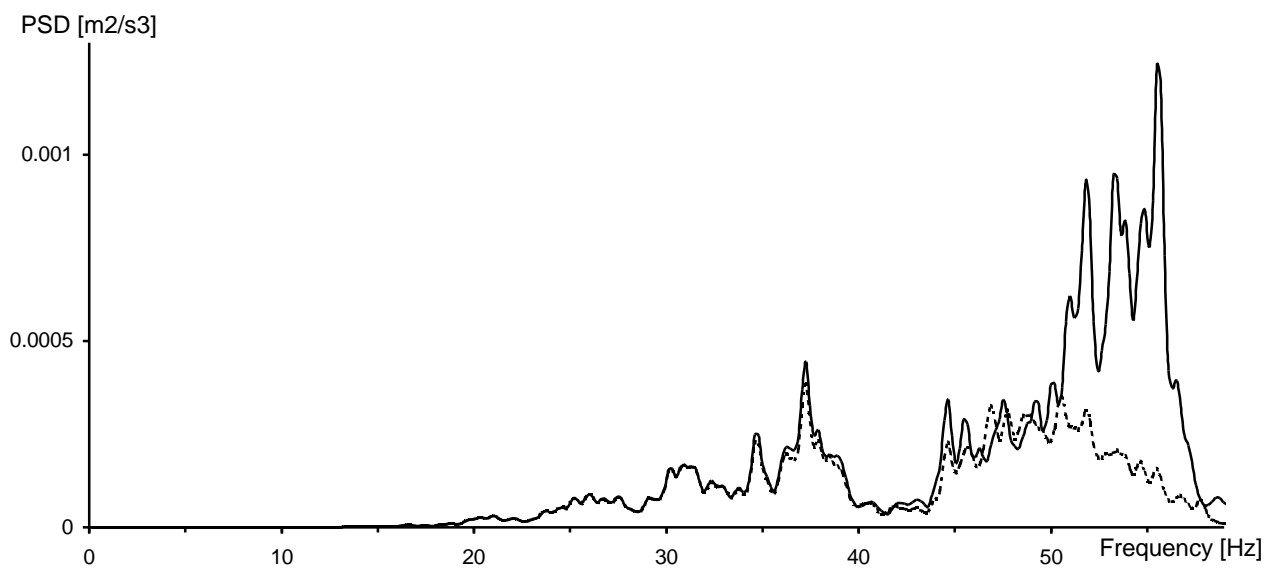
However, the situation changes if one compares the road data and the synthetic background signal not in frequency domain but in terms of time history or probability distribution of instantaneous values. Figures 5,a,c and 6,a,c show time histories for wavelet groups No 2 and No 1 for the road data. The low amplitude instantaneous values of the above signals have been eliminated from the time histories so as to focus on the higher amplitude peaks larger than a certain limit. To obtain statistically representative material about bump events happening rarely, acquisition of road vibration signals should be much longer than in the case of ordinary PSD analysis. Therefore, the above graphs include data from 20 repetitions of the aforementioned one-minute run of the vehicle, which all were made on the same track and then placed one by one into the joint record. When synthetic Fourier signal was presented in the same view (Figs. 5,b,d and 6,b,d) it became clear that for wavelet group No 1 the road data regularly exhibit bumps of such a height and frequency of appearance which are absent in the Fourier signal of the same group. The same result has been also obtained for the group No 3. This is not the case for group No 2 (see Fig. 5) and group No 4 as well whose behaviour in terms of bump events is similar for the road data and for the synthetic Fourier signal.



a) PSD of mildly nonstationary road data and synthetic Fourier background signal

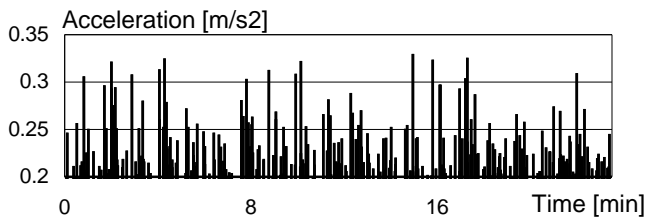


b) PSD of 2nd wavelet level (dotted curve) and wavelet group No 1 for road and Fourier signals (solid curves)

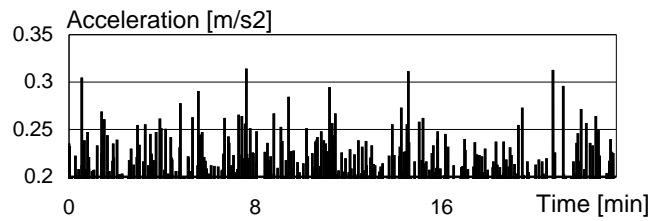


c) PSD of 3rd wavelet level (dotted curve) and wavelet group No 1 (solid curve) for road data

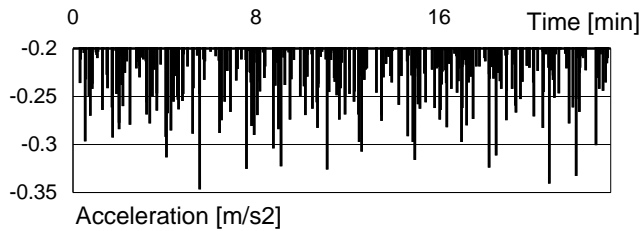
Fig. 4 Wavelet level grouping and comparison of PSDs of road data and mission background signal.



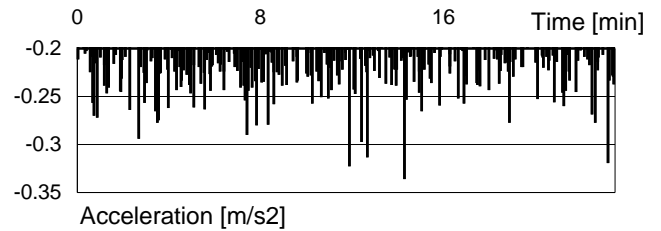
a) Road data positive peaks



b) Fourier simulation positive peaks

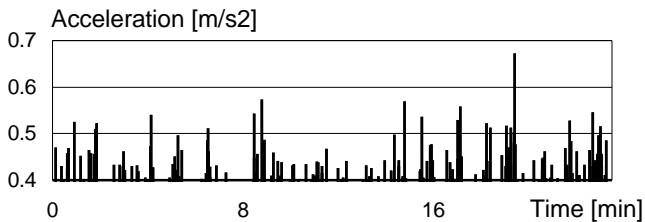


c) Road data negative peaks

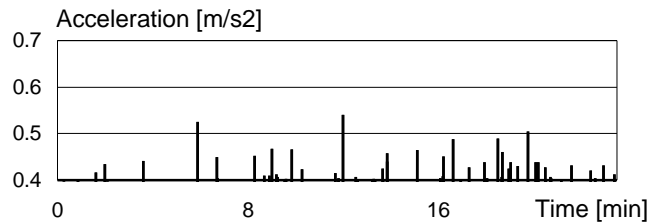


d) Fourier simulation negative peaks

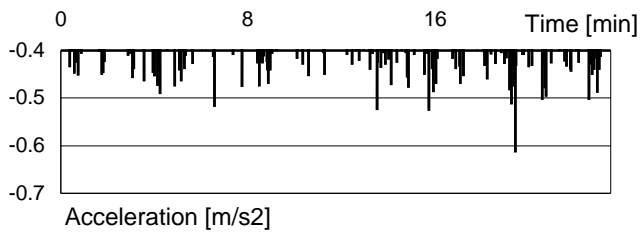
Fig. 5 Time history peaks for the wavelet group No 2.



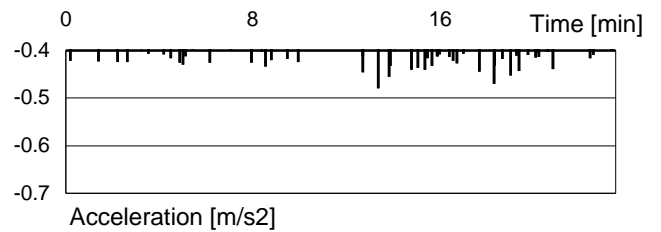
a) Road data positive peaks



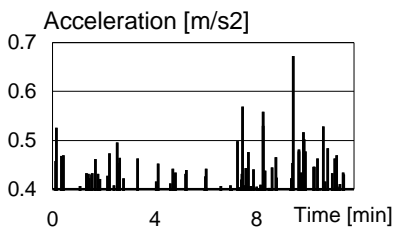
b) Fourier simulation positive peaks



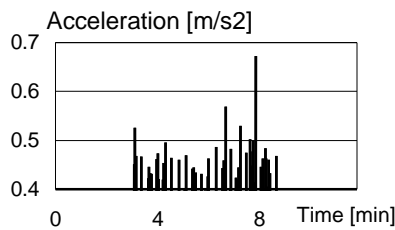
c) Road data negative peaks



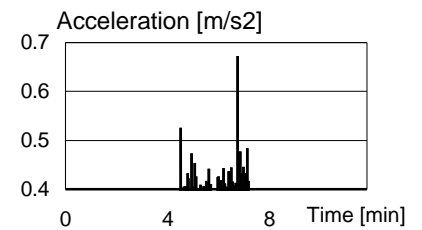
d) Fourier simulation negative peaks



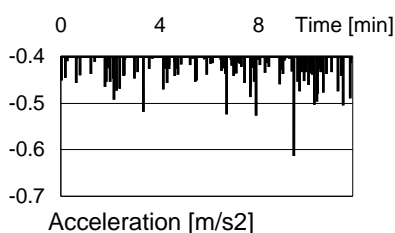
e) 1/2 length mission positive peaks



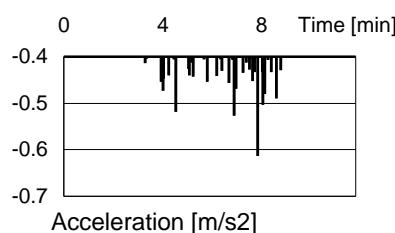
f) 1/4 length mission positive peaks



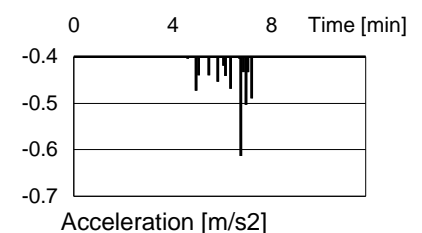
g) 1/8 length mission positive peaks



h) 1/2 length mission negative peaks



i) 1/4 length mission negative peaks



k) 1/8 length mission negative peaks

Fig. 6 Time history peaks for the wavelet group No 1.

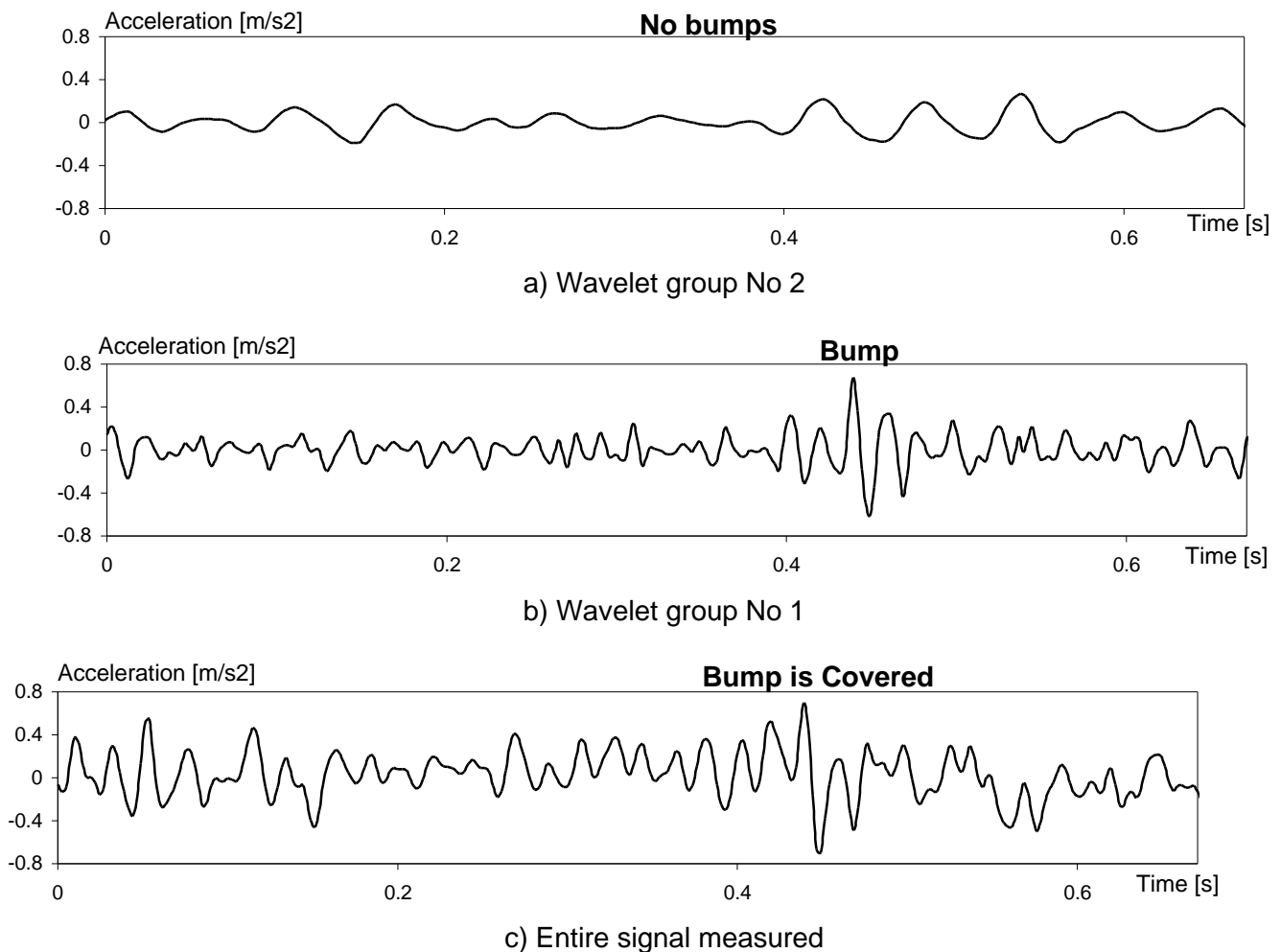
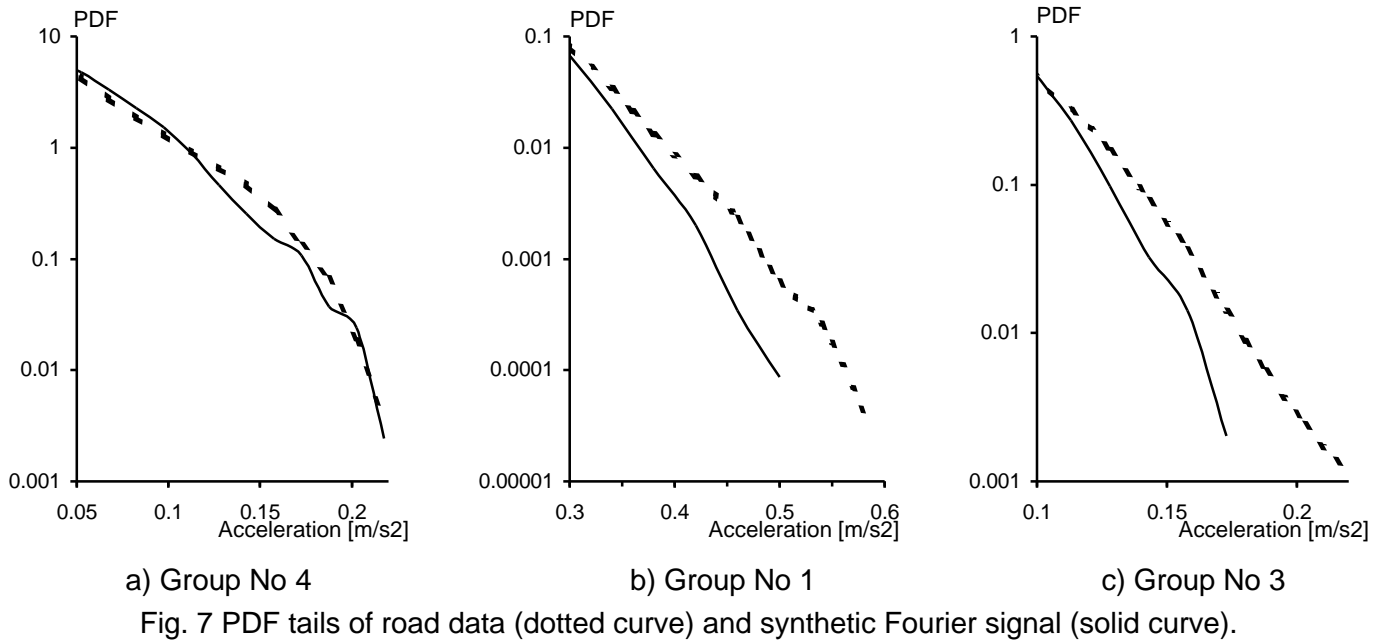


Fig. 8 Time histories of road data with a bump event related to higher chassis resonances or tire resonances

Evaluation of the above time history graphs with amplitude region for positive and negative peaks magnified is somewhat subjective and requires operation with very long time history files. Therefore, another view to the problem under consideration may be recommended making use of probability density function (PDF) and, particularly, of its tail behaviour describing probability of large instantaneous values, i.e. how often these large peaks appear in the time history. In Fig. 7, where a logarithmic scale is used for vertical axis to represent low probability values better, the dotted curve is obtained by averaging left and right PDF tails of one of the four wavelet groups of the road data. Solid curves showing results of the same analysis made for the synthetic

Fourier signal are close to the dotted curves of the road data for the wavelet groups No 2 and No 4 (the latter is presented in Fig. 7,a). On the other hand, for groups No 1 and No 3 the PDF tails of the synthetic signal always lie lower than those of the road data (see Fig. 7,b,c) whose PDF tails are wider and longer. It means that a peak of the same height from the region of about 3 RMS values and more, presented on the horizontal axis, has several times less probability of appearance in synthetic Fourier signal than in the road data.

5. Extraction of bump events from road data and construction of vibration mission

The above result of comparison of the road and synthetic Fourier data reveals difference in bump behaviour, that is a matter of concern in the paper. This suggests that specific action for the purpose of bump modeling should be undertaken for certain wavelet level signals in addition to conventional PSD simulation. Other wavelet levels, where there is no essential bumps, can be left in the form resulted from Fourier simulation and, then, immediately included in the summation signal during reconstruction of vibration mission.

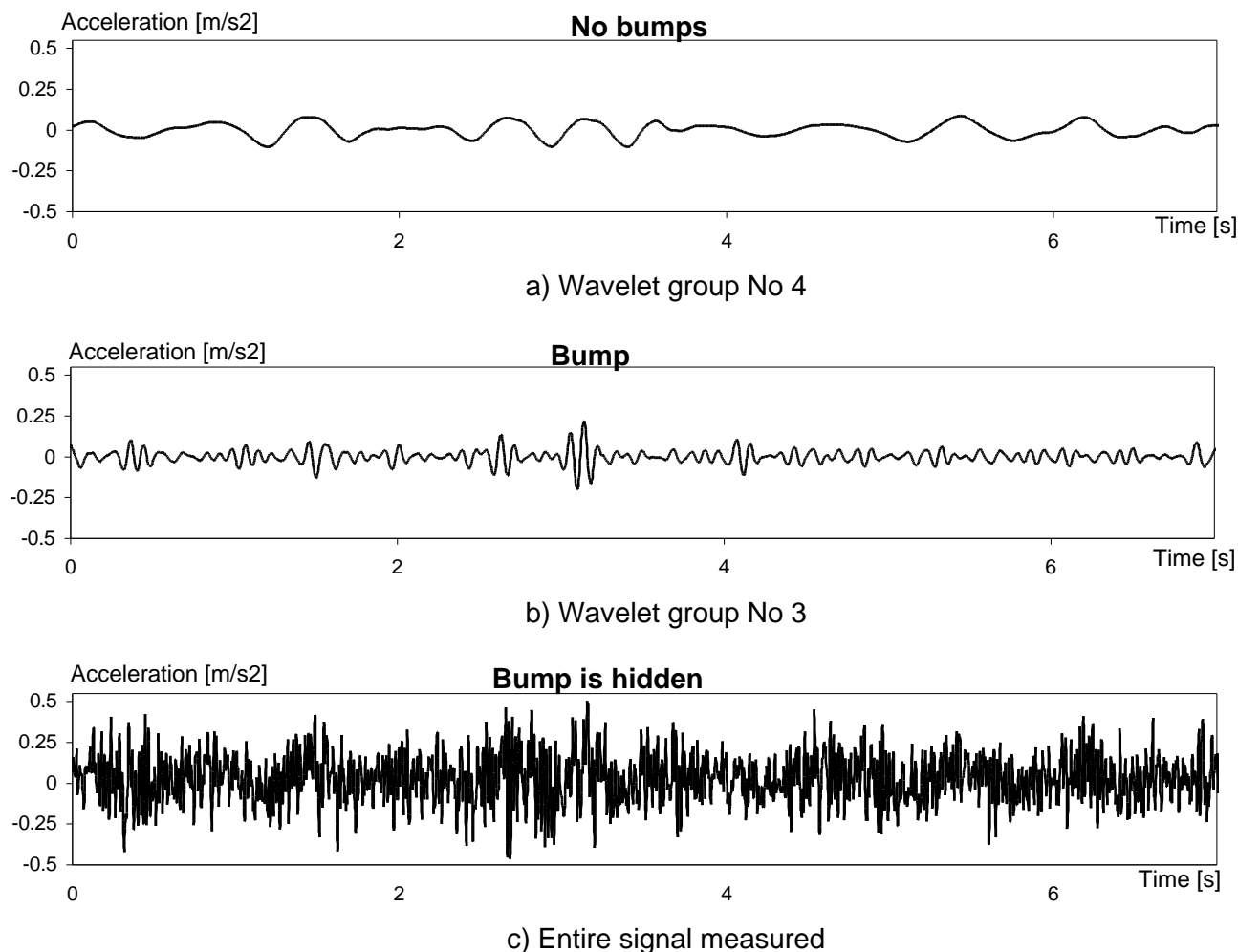


Fig. 9 Time histories of road data including a bump event related to suspension resonances or the rigid body motion of the engine/gearbox

The usefulness of the wavelet decomposition for identifying bump events is illustrated by Figs. 8 and 9. One of the bumps observed in the time history of wavelet group No 1 is presented in Fig. 8,b. It is there because something relevant happened at this moment of time in the frame of that physical phenomenon which is related to the wavelet group under consideration. At the same time there is nothing to cause bumps in the frame of other physical phenomenon related to another wavelet group (for example group No 2 shown in Fig. 8,a) and its contribution to the road signal covers the above bump making it much less distinguishable in the time history of the entire road data (see Fig. 8,c). This situation is typical and was also observed for wavelet levels with lower frequency content when wavelet group No 4 had no bumps (Fig. 9,a) whereas group No 3 did have one (Fig. 9,b). However, in the entire signal (Fig. 9,c) the latter was not only less obvious, as it was the case for previous example shown in Fig. 9,c, but the bump was absolutely hidden and could not be revealed at all without wavelet decomposition.

Thus, each of the wavelet groups defined on the second stage of the proposed procedure established in Section 3 of the paper was being considered separately. Going along the time history point by point the

algorithm was looking for bump events formalised according following mathematical criterion. A point is considered indicative of bump event if at the same moment of time the road data signal has maximum or minimum and the wavelet group time history exceeds certain boundary value which is prescribed so that can be reached only by high peaks in the time history. Experience suggested that this boundary value expressed in terms of crest factor may be taken equal to 3.5 times RMS value. Assuming that any bump event takes some time to be developed from background vibration and, then, must be accompanied by some decay process depending on dumping in the system, the main peak found in road data and taken to the vibration mission should be accompanied by a few preceding and subsequent waves.

When a bump event is identified in the wavelet group of the road data it should be placed to the same wavelet group of the synthetic Fourier signal with minimum disturbance to the latter. For this purpose the time history section with a bump is moved along the whole time history of the synthetic signal and compared with it in terms of root-mean-square difference in each of possible positions. Then, at the point where this difference appeared to be of the smallest value, the bump section substitutes the similar and equal in length section found in the background synthetic signal upgrading it into vibration mission when this is done for all bump events identified in the current wavelet group of the road data. To confirm that action of superimposing bumps on the background Fourier signal has not affected simulation in the frequency domain, PSDs of wavelet groups No 1 and 3 for the constructed vibration mission are shown in Fig. 10 and compared with the same for the initial road data.

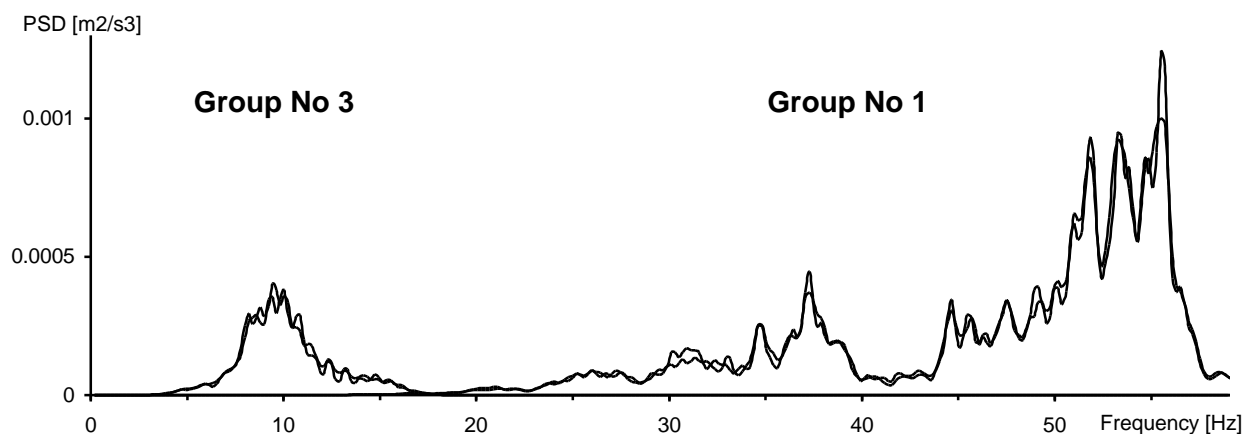


Fig. 10 PSD of wavelet groups No 1 and No 3 for vibration mission and road data

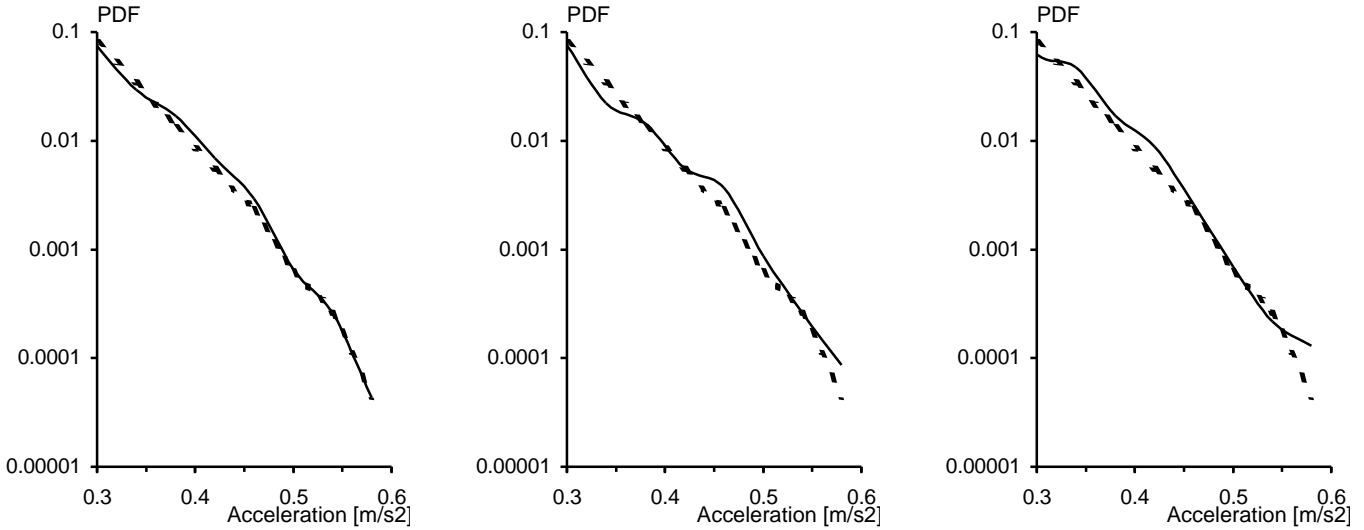
The number of bump events identified in the wavelet group can be a simple criterion while taking a decision whether the particular wavelet group of the Fourier signal is similar to that of the road data or it is necessary to move bumps from the road to synthetic time history. Certainly it would be the best to make the comprehensive analysis of PDF tails or compressed and clipped time histories as it is shown in previous section of the paper. However, for engineering applications or in order to make the procedure automatic and suitable for inclusion in a computer algorithm, a simpler rule in the form of one numerical index may be needed. To illustrate development of such a simple criterion, the Table presented below contents number of bump events obtained in road and synthetic Fourier data for all four wavelet groups during about 12 minutes recording time. Evaluating ratios between the numbers of bump events in the road and synthetic data one can see that for wavelet groups No 1 and No 3 this ratio is 2.5 and 3.0 correspondingly. It means, as it was found in previous section of the paper, that in these wavelet groups bump events appear much frequenter for the road data than for the synthetic Fourier signal. From the other hand for wavelet groups No 2 and No 4, which have been classified as not representative of bump events, the ratio is 1.5 and 1.0 correspondingly. These results allow to introduce 2.0 as a value of trigger ratio for running the above procedure of moving bump events from road data to the same wavelet group of the synthetic Fourier signal.

Wavelet group No	1	2	3	4
Number of bump events in road data	365	122	151	15
Number of bump events in Fourier signal	150	78	51	14
Ratio of the above two lines (rounded off)	2.5	1.5	3.0	1.0

Before this point it was assumed that all bump events found in road data are moved to the synthetic Fourier signal to make statistical characteristics of the obtained vibration mission most close to those of the road data. However, as mentioned in Introduction, the vibration mission may be requested to be several times shorter than the data record collected in road experiments. If all bump events extracted from road data were introduced to the shorter vibration mission, the latter would inevitably become overdosed with bump events

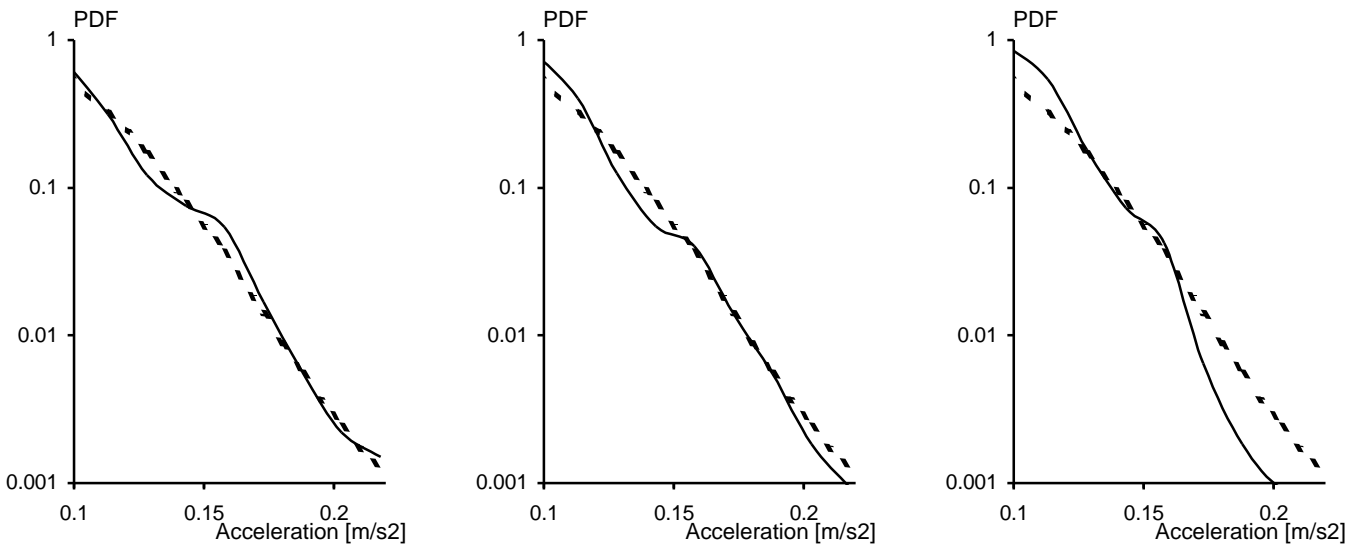
and, therefore, more harmful for a human than real road excitation is. To construct vibration mission with characteristics similar to the prescribed road record while being n -times shorter, one should take not all but n -times less number of bump events from those extracted from the whole record of road data.

This was done in the developed algorithm by, first, ranking all found bumps in descending order according their main peak value and, second, picking up the bumps for vibration mission from this sequence with a step equal to compression value n . In so doing bump events of various intensity will appear in the mission. Each of them will be also a representative of $(n-1)$ other bumps of close height not included into the vibration mission. Closeness of road and mission statistical characteristics is ensured by the fact that probability of appearance of a particular bump existing in the vibration mission is equal to joint probability of appearance of n bumps of similar height in the road record which is n -times longer than the vibration mission.



a) Vibration mission of 1/2 length b) Vibration mission of 1/4 length c) Vibration mission of 1/8 length

Fig. 11 PDF tails of road data (dotted curve) and vibration mission (solid curve) for wavelet group No 1.



a) Vibration mission of 1/2 length b) Vibration mission of 1/4 length c) Vibration mission of 1/8 length

Fig. 12 PDF tails of road data (dotted curve) and vibration mission (solid curve) for wavelet group No 3.

Results of checking closeness of PDF tails for the road data (dotted curves) and for the vibration missions 2 times, 4 times and 8 times shorter (solid curves) are presented in Figs. 11 and 12. The conclusion is that a discrepancy between probability distribution tails of road data and synthetic signals for wavelet groups No 1 and No 3, which existed after the Fourier simulation stage in the mission construction process (see Figs. 7,b,c), disappeared after the second stage of extracting bumps from the road data and the third stage of superimposing them on the Fourier signal background had been performed. It should be mentioned that the results for wavelet group No 3 seem worse than for group No 1 and for larger compression values worse than for lower ones not because there is a real reason of that but because statistical material (number of bump events per the record length unit) available for PDF analysis was smaller for the group No 3 than for the group No 1 and, obviously, was the smaller the large is the compression value.

An improvement in simulation of bump behaviour can be also evaluated by a simpler than PDF analysis numerical criterion which is the kurtosis value (2) because, as was mentioned in Section 2, it is sensitive to outlying points among instantaneous values of the signal under consideration. For wavelet group No 1 the kurtosis value of the road data was $g=3.39$ whereas for the synthetic Fourier signal at the first stage of mission construction it was less, particularly $g=3.02$. After operation with bump events and completion of the developed procedure the kurtosis raised to appropriate value $g=3.32$. For wavelet group No 3 the similar figures were following: $g=4.0$ – for the road data, $g=3.26$ – for the synthetic Fourier signal and $g=3.76$ – for the vibration mission constructed.

To assess results of mission construction algorithm in the time domain one can evaluate time history plots in Figs 6,e-k for wavelet group No 1. Although being shorter two, four, or even eight times than the road data record shown in Figs. 6,a,c these compressed vibration missions, which were constructed by the mission synthesis algorithm developed, look very similar to the road data. This is not the case for the results (Figs. 6,b,d) of common Fourier simulation procedure which does not take into consideration bump events happening on the road and making the measured vibration to be of mildly nonstationary nature. To reconstruct an entire vibration mission to be used as an input signal for human factors test benches or in computer simulation, one need to summarize all synthetic wavelet group signals just as corrected with bumps, like groups No 1 and No 3 in the considered example, so also those (particularly No 2 and No 4) left unchanged after initial Fourier generation in frequency domain.

6. Conclusions

The developed algorithm uses Fourier analysis, orthogonal Daubechies 12 wavelets and peak correction procedures with crest factor control to condense experimentally measured vibration data into short test sequences which are representative of the original record in statistical terms. Compression ratios of up to 8 have been achieved without compromising the statistical quality of the resulting mission signal for a vibration data set from a Renault automobile. Analysis is continuing using data sets from a heavy industrial lorry and from other automobiles in order to establish what average and what maximum compression ratios can be expected from typical data. Future extensions of the procedure include the addition of a stage which can classify and analyse nonstationary data structures such as shocks, so as to provide a complete documentation of the road features found in the data.

Acknowledgements

The research described in this paper was financed by the European Commission as part of the activities of Brite-Euram Project BE-97-4186 SCOOP "Seat Comfort Optimisation Procedure". The authors would like to express their gratitude to Mr. Mohamed Karouia of Renault Technocentre for providing the experimental data and for aiding in data interpretation.

References

- [1] Daubechies, I. 1992, Ten lectures on wavelets, SIAM, Philadelphia, PA.
- [2] Giacomini J. and Bracco R. 1995, An experimental approach for the vibration optimisation of automotive seats, ATA 3rd Int. Conf. on Vehicle Comfort and Ergonomics, Bologna, Italy, March 29-31
- [3] Giacomini, J., Scarpa, F. and Caretto, L. 1998, Some observations regarding the nonlinearity of person/seat frequency response functions, Int. Conf. on Noise and Vibration Eng. (ISMA 23), Leuven, Belgium, Sept. 16-18
- [4] Meyer, Y. 1993, Wavelets. algorithms & applications, SIAM, Philadelphia, PA.
- [5] Newland, D.E. 1993, Random vibration, spectral and wavelet analysis, 3rd edition, Longman, Harlow and John Wiley, New York.
- [6] Staszewski, W.J. 1998, Wavelet based compression and feature selection for vibration analysis, Journal of Sound and Vibration, Vol. 211, No. 5, pp. 735-760.
- [7] Staszewski, W.J. and Giacomini, J. 1997, Application of the wavelet based FRF's to the analysis of nonstationary vehicle vibration, 15th Int. Modal Analysis Conf. IMAC, Orlando Florida, U.S.A., Feb 3-6
- [8] Shinozuka, M. and Jan C.-M., 1972, Digital simulation of random processes and its applications, *Journal of Sound and Vibration*, Vol. 25, pp. 111-128.
- [9] Vandeurzen, U., Leuridan, J., Mergeay, M., et al., Versatile computer workstation for multiple input/output structural testing and analysis, *Proc. of 18th Int. Symp. on Automotive Technology and Automation*, Florence.